Poly(3-hydroxybutyrate)-ethyl cellulose based bio-composites with novel characteristics for infection free wound healing application

Hafiz M.N. Iqbal[1]
Godfrey Kyazze[1]
Ian Charles Locke[1]
Thierry Tron[2]
Tajalli Keshavarz[1]

[1] Faculty of Science and Technology, University of Westminster, London, UK
[2] Aix Marseille Université, CNRS, Centrale Marseille, France, UK

Poly(3-hydroxybutyrate)-ethyl cellulose based bio-composites with novel characteristics for infection free wound healing application

Hafiz M. N. Iqbal[a,*], Godfrey Kyazze[a], Ian Charles Locke[a], Thierry Tron[b] and Tajalli Keshavarz[a,*]

[a] Applied Biotechnology Research Group, Department of Life Sciences, Faculty of Science and Technology, University of Westminster, London, United Kingdom; [b] Aix-Marseille Université, CNRS, Centrale Marseille, iSm2 UMR 7313, 13397 Marseille, France. *Corresponding author, Tel.: +44 020 79115030; fax: +44 020 79115087; E-mail addresses: hafiz.iqbal@my.westminster.ac.uk (H.M.N. Iqbal) and t.keshavarz@westminster.ac.uk (T. Keshavarz)

Abstract

A series of bio-composites including poly3-hydroxybutyrate [P(3HB)] grafted ethyl cellulose (EC) stated as P(3HB)-EC were successfully synthesised. Furthermore, natural phenols *e.g.*, *p*-4-hydroxybenzoic acid (HBA) and ferulic acid (FA) were grafted onto the newly developed P(3HB)-EC-based bio-composites under laccase-assisted environment without the use of additional initiators or crosslinking agents. The phenol grafted bio-composites were critically evaluated for their antibacterial and biocompatibility features as well as their degradability in soil. In particular, the results of the antibacterial evaluation for the newly developed bio-composites indicated that 20HBA-*g*-P(3HB)-EC and 15FA-*g*-P(3HB)-EC bio-composites exerted strong bactericidal and bacteriostatic activity against Gram$^-$ *E. coli* NTCT 10418 as compared to the Gram$^+$ *B. subtilis* NCTC 3610. This study shows further that at various phenolic concentrations the newly synthesised bio-composites remained cytocompatible with human keratinocyte-like HaCaT skin cells, as 100% cell viability was recorded, *in vitro*. As for the degradation, an increase in the degradation rate was recorded during the soil burial analyses over a period of 42 days. These findings suggest that the reported bio-composites have great potential for use in wound healing; covering the affected skin area which may favour tissue repair over shorter periods.

Keywords: Ethyl cellulose; Bio-composite; HaCaT compatible

1. Introduction

Cellulose is the most abundant renewable material widely used in the history of mankind. In recent years, with the increasing knowledge of infectious diseases caused by various micro-organisms, the development of bio-polymers with multi-functional properties has gained considerable attention, especially in bio-medical and other health-related areas of the modern world. Furthermore, preparations of such structured

materials in the form of composites by combining the advantage of various biopolymers like cellulose are among potential routes to impart and/or modify existing properties of natural polymers [1]. Over the last few years, many polymer researchers have directed their interests into the development of structured materials with multi-functional characteristics for wider range of applications like bio-medical, pharmaceutical, drug delivery, antibacterial active packaging and/or sanitary materials, and household items [2].

In our previous work, P(3HB)-EC-based novel composites were developed and analysed the improved thermo-mechanical characteristics and hydrophobic and/or hydrophilic balance obtained [3]. Most phenols, as natural antimicrobial agents, can be grafted onto cellulose surface to impart antimicrobial properties. The cross-linking behaviours of various phenolic molecules including HBA was evidenced after treatment with laccase from *Pycnoporus cinnabarinus* and others [4, 5].

Laccase-assisted grafting has recently been the focus of green chemistry technologies in response to the growing environmental concerns, legal restrictions and advances in science. In principle, laccase-assisted grafting may modify and/or impart a variety of new functionalities to the materials of interest, as the modified materials through grafting have extensive applications [6-8]. Oxidoreductases like laccase have considerable potential to react with a large variety of suitable substrates *e.g.*, phenols. This is because their redox potentials are sufficiently low to allow electron transfer by Cu1 reaction site of the laccase. Over the last few decades laccases have been established as green catalysts. There is special interest on laccases due to their ability to generate phenoxy radicals as the primary oxidation products. These radicals can further undergo cross-linking reactions [9-11], thus enhancing/modifying characteristics of existing material, and/or imparting new features to the materials, creating value-added products. Laccase-assisted bio-grafting is a versatile method of functionalisation, which allow bonding of various functional groups from diverse phenolic structures [2, 12].

The tested phenolic structures have pronounced antibacterial features against various bacterial strains, and exert strong pharmacological activities such as flavouring, antioxidant and antiseptic characteristics, has already been reported elsewhere [13, 14]. In continuation of our previous study [3], herein, we report a new study on the development of bio-composites with novel characteristics through enzymatic grafting.

2. Materials and Methods

2.1. Chemicals

The enzyme used for grafting purposes was a commercial laccase from *Trametes versicolor* (Sigma-Aldrich, UK). 2,2'-azino-bis(3-ethylbenzothiazoline-6-sulphonic acid) (ABTS) and natural phenols *i.e.*, *p*-4-

hydroxybenzoic acid and ferulic acid were supplied by Sigma-Aldrich, UK. Dulbecco's modified eagle's medium (DMEM), phosphate buffer saline (PBS), streptomycin and penicillin were provided by Lonza, Wilford Industrial Estate, Nottingham UK. Fetal calf serum was from Labtech International Ltd., Bellbrook Industrial Estate, East Sussex UK.

2.2. Stock cultures

$Gram^+$ and $Gram^-$ bacterial strains *i.e., Bacillus subtilis* NCTC 3610 and *Escherichia coli* NTCT 10418, respectively were obtained in their pure form the University of Westminster's bacterial culture collection unit. Both of the collected strains were streaked on sterile nutrient agar plates which were then used to prepare inoculum suspension. A homogenous spore suspension was grown, separately, in 50 mL sterile nutrient broth for 24 h at 30 °C and 120 rpm.

2.3. Grafting of HBA and FA

The grafting of HBA and FA onto the previously developed P(3HB)-EC composite [3] was performed. Briefly, a pre-weight composite was dipped in a glass basin containing 50 mL of pre-dissolved HBA and FA, separately, in the presence of laccase for 60 min at 30 ^oC. The control sample [P(3HB)-EC] was treated in the same way using sodium malonate buffer alone without adding HBA and FA. After 60 min, the weight of each composite was recorded in the swollen state followed by incubation at 50 ^oC until fully dried. Afterwards, each of the composite was washed three times with sodium malonate buffer to eliminate any of the unreacted HBA and FA, and then again dried at 50 ^oC and final dry weight was recorded to calculate the grafting parameters. Laccase was assayed by monitoring ABTS oxidation method (ε_{420}= 36000$M^{-1}cm^{-1}$) and the activity was found to be negligible at the end of the experiment. All of the samples were prepared in triplicates and for each treatment means ± S.E. were calculated.

2.4. Structural and elemental evaluation (FT-IR)

To investigate the structural and elemental groups of the grafted composites along with their individual counterparts, an FT-IR spectroscopy was used. Prior to record the spectra, the test composites were placed directly on the diamond crystal of a Perkin Elmer System 2000 FT-IR spectrophotometer. An IR absorption spectra were recorded using the wavelength ranging from 4000 to 500 cm^{-1}.

2.5. Grafting parameters

The effect of different phenolic concentrations on the grafting process was investigated in terms of grafting parameters. The grafting parameters were calculated according to the following equations as reported earlier [15].

$$\% \text{ Graft yield} = \frac{Wf - Wi}{Wi} \times 100 \quad (1)$$

$$\% \text{ Grafting efficiency} = \frac{Wf - Wi}{Ws - Wi} \times 100 \quad (2)$$

$$\% \text{ Swelling ratio} = \frac{Ws - Wi}{Wi} \times 100 \quad (3)$$

Where, Wi = initial weight; Wf = final dry weight; and Ws = weight in swollen state

2.6. Testing antibacterial activity

A conventional spread-plate method was adopted to evaluate the antibacterial characteristics of the newly synthesised composites. The antibacterial characteristics were tested verses *B. subtilis* NCTC 3610 and *E. coli* NTCT 10418 strains, *in vitro*. All of the grafted composites were thermally sterile at 90 ^{o}C for 30 min prior to inoculate the overnight grown bacterial spore suspensions (containing 10^5 CFU/mL) on the surfaces of the test composites. After 24 h incubation, the bacterial cells from the control and test composites were washed twice using 50 mL phosphate buffer (pH, 7.0). The bacterial cell count in terms of CFU/mL was determined by conventional spread-plate method. In comparison with control the CFU/mL values were used to calculate the antibacterial efficacy of the test composites using Eq. 4.

$$\text{Log reduction} = \text{Log CFU Control sample} - \text{Log CFU Treated sample} \quad (4)$$

2.7. *In vitro* biocompatibility

HaCaT cell line was adopted to evaluate the biocompatibility of the newly synthesised composites. The newly synthesised bio-composites with 1 cm^2 in area were cut, UV sterilised and then HaCaT cells were seeded at a density of 1×10^5 cells per well. The seeded composites were incubated at 37 ^{o}C in a humidified atmosphere of 5% CO_2. After 1, 3 and 5 days of incubation, the growth media were removed from each well and PBS was used to rinse each composite three times. The percentage cell viability was recorded using neutral red dye uptake assay. After 3 h of incubation under standard assay conditions, the test composites were washed three times using mixture contained $CaCl_2$ and formaldehyde with a percent range of 1 % and 0.5 %, respectively. This was then followed by 10 min incubation at an ambient temperature using lysate mixture in order to extract the taken up dye by the viable cells. From above, 100 µL was transferred to 96-well cell culture plates and OD value was measured using a Thermomax micro-plate reader at 540 nm using Softmax Pro version 4.8 software. The % cell viability of the test specimens was calculated using Eq. 5.

$$\% \text{ HaCaT viability} = \frac{\text{OD Test composite} - \text{OD Negative control}}{\text{OD Positive control}} \times 100 \quad (5)$$

Standard tissue culture plastic was used as positive control whereas graft composite without cell culture was used as negative control for this experiment.

2.8. Adherent Morphology

The adherent morphology was observed using Nikon light microscope. After stipulated incubation days, the HaCaT cells were fixed for 30 min using mixture solution contained paraformaldehyde and PBS with a percent range of 4% and 96%, respectively. The samples were washed with PBS and then followed by adding 5 mg/mL neutral red dye to stain HaCaT cells for 1 h. After the stipulated time, the stained cells were washed with PBS and high definition images at 100× were captured using ScopePhoto, Windows based software version x86, 3.1.475.

2.9. Biodegradability

The biodegradability of the composites as a function of time-dependent weight loss was performed as described earlier by Wattanakornsiri et al. [16], with minor modifications as reported earlier [15]. The percentage of weight loss was calculated using Eq. 6.

$$\% \text{ loss in weight} = \frac{\text{Control weight} - \text{Loss in weight}}{\text{Control weight}} \times 100 \qquad (6)$$

3. Results and Discussion

3.1. Structural and elemental evaluation (FT-IR)

A typical FT-IR spectra of the individual *i.e.*, HBA, FA and P(3HB)-EC and their laccase-assisted HBA-*g*-P(3HB)-EC and FA-*g*-P(3HB)-EC bio-composites is shown in Fig. 1A and B, respectively. IR spectral profile of the HBA-*g*-P(3HB)-EC was different in comparison to that of the pristine HBA profile. The appearance of strong peaks at 1,689 and 1,607 cm^{-1} regions are accredited to C=O and COO^- vibrations of HBA and HBA-*g*-P(3HB)-EC moieties, respectively. The bands at 1,446 and 1,240 cm^{-1} wavelength region are accredited to in-plane hydrogen bonding, which are shifted to 1,360 and 1,056 cm^{-1} in the spectrum of the HBA-*g*-P(3HB)-EC composites. Whereas, the bands in the fingerprint region 3,070-2,860 cm^{-1} region are due to the aromatic and hetero aliphatic rings (Smith and Dent 2005). FT-IR spectra of FA and FA loaded P(3HB)-EC bio-composites (Fig. 1B) showed significant -OH (3,350 cm^{-1}) and aliphatic (2,800-3,000 cm^{-1}) bands and accredited to C–H, CH_2 and CH_3 vibrational modes [17]. Between 1,500 and 1,720 cm^{-1} wavelength regions, there are bands at 1,720 cm^{-1} due to C=O, 1,680 cm^{-1} due to ketones and 1,510 cm^{-1} due to single aromatic ring which is a characteristic feature of FA. In this region, there may also be contributions from aromatic functional groups and molecular water. C–H deformations occur at 1,440 cm^{-1} and C–O stretches dominate the region

1,050-1,300 cm^{-1}. The grafted bio-composites have typical polyphenol attributes, due to the appearance of broad peaks cantered at 3,346 and 1,446 cm^{-1} which are assigned to the vibrational mode of O-H linkages of phenolic and hydroxyl groups. In comparison to the pristine HBA and FA spectra a sharp peak at 1,056 cm^{-1} region appeared in the FT-IR spectra of HBA-*g*-P(3HB)-EC and FA-*g*-P(3HB)-EC bio-composites and mainly corresponds to C-O-C mode, indicating extended polymerisation [6, 18].

3.2. Grafting parameters

Figure 2A and B shows the effect of HBA and FA concentrations on the grafting parameters. A consistent increase in the grafting parameters was recorded up to 20 mM HBA concentration. Indeed, the grafting parameters profile presented in Fig. 2A indicates that as the concentration of HBA increases from 0 to 20 mM both the %GY and %GE were optimal with an increase in the swelling ratio. Figure 2B depicting the aforementioned grafting parameters of FA-*g*-P(3HB)-EC bio-composites. The data revealed that the graft yield, grafting efficiency and swelling ratio values were maximum in case of 15FA-*g*-P(3HB)-EC, then starts to decrease showing that higher concentrations do not promote further grafting. One possible reason for the observed behaviour could be the substantial amount of FA grafted onto the backbone material, which creates steric hindrance for further grafting on increasing beyond the optimal point. The method employs laccase to convert the phenol used, HBA and FA, into free radicals, which undergoes subsequent non-enzymatic reaction with the backbone composite and thus forms graft composite. Graft copolymerisation using free radical initiation has attracted the interest of many scientists in the last few years. In an earlier study, Sun et al. [19] prepared carboxymethyl chitosan-grafted-MAA composites using free radicals in an aqueous solution and observed that the reaction time and temperature are among important parameters which can increase or decrease the grafting parameters such as graft yield, grafting efficiency and swelling behaviour. Similarly, Kumar et al. [20] and Chen et al. [21] have also used enzyme as a catalyst for grafting purposes. Previously, Aggour, [22] has also observed the similar phenomenon with an increase in the grafting percentage due to the increase in monomer concentration, which in turn also intensify the molecular weight of the grafted composite.

3.3. Antibacterial activity

The antibacterial activities of HBA-*g*-P(3HB)-EC and FA-*g*-P(3HB)-EC bio-composites were tested against *B. subtilis* NCTC 3610 and *E. coli* NTCT 10418 and the results obtained are shown in Fig. 3A and B, respectively. After 24 h of incubation, a significant bacterial proliferation with an increase in the log value from 5 to 8 and 6 against *B. subtilis* NCTC 3610 and *E. coli* NTCT 10418, respectively was recorded on control composite. In contrast, 15HBA-*g*-P(3HB)-EC and 20HBA-*g*-P(3HB)-EC bio-composites, prepared with 15 mM

and 20 mM HBA concentration respectively, showed a clear bacteriostatic and bactericidal effects against *B. subtilis* NCTC 3610 and *E. coli* NTCT 10418, respectively. Whereas, 5HBA-*g*-P(3HB)-EC and 10HBA-*g*-P(3HB)-EC bio-composites were not as effective particularly against *B. subtilis* NCTC 3610. However, both composites showed a significant bacteriostatic activity against *E. coli* NTCT 10418 with a log reduction value from 5 to 2 and 1, respectively. The total log reduction value caused by 20HBA-*g*-P(3HB)-EC bio-composite for *E. coli* NTCT 10418 and *B. subtilis* NCTC 3610 was 0 and 2, respectively in comparison to the control log value *i.e.*, 5. On the other hand, in case of FA grafted composites a significant antibacterial activity was detected for 15FA-*g*-P(3HB)-EC against $Gram^+$ strain *i.e., B. subtilis* NCTC 3610 and $Gram^-$ *i.e., E. coli* NTCT 10418 in comparison to the control sample and also relative to the other FA grafted bio-composites. Furthermore, 10FA-*g*-P(3HB)-EC was found more bacteriostatic, as compared to the 5FA-*g*-P(3HB)-EC and 20FA-*g*-P(3HB)-EC bio-composites, against both of the aforementioned strains. Generally, the bactericidal potential against $Gram^-$ *E. coli* NTCT 10418 was higher than that of $Gram^+$ *B. subtilis* NCTC 3610 at the same composite, which is, probably because of the difference between $Gram^-$ and $Gram^+$ bacteria in terms of cell structures [23, 24]. According to the data discussed above, the antibacterial potential of the newly grafted composites was due to the HBA and FA as functional entities. It is well-known that the antibacterial mechanism or bacteriostatic and bactericidal potential of phenols, such as HBA and/or FA, is natural which is due to the availability of reactive acidic hydroxyl groups in their structure. Further to this end, it has also been reported in literature that the delocalisation of electrons on their structure also contribute to their antibacterial mechanism or bacteriostatic and bactericidal potential against various bacterial strains [11, 25].

3.4. *In vitro* biocompatibility

In recent years, cellulosic-based composites have been widely employed in various sectors of current biomedical fields. Owing to some previously characterised and reported characteristics of the P(3HB)-EC composite [3], the newly grafted composites, *i.e.*, HBA-*g*-P(3HB)-EC and FA-*g*-P(3HB)-EC, are expected to exhibit an excellent HaCaT compatibility. Notably, no matter low or higher HBA and/or FA concentrations, HBA-*g*-P(3HB)-EC and FA-*g*-P(3HB)-EC bio-composites displayed increasing cell viability among the tested composites, whereas, 20HBA-*g*-P(3HB)-EC (Fig. 4A) and 15FA-*g*-P(3HB)-EC (Fig. 4B) composites showed 100% cell viability after 5 days of incubation, indicating that these composites were non-cytotoxic under *in vitro* cell culture conditions. Additionally, the morphologies of cell cultured from all of the test composites displayed healthy shape (Figs. 5 and 6). With the extension of culture time from day 1 to day 5 the number of cells

attached on the seeded composite surfaces was increased. It could be seen from Figs. 5 and 6, the HaCaT cells adhered on the composites and spread in a stretchy way on their surfaces.

3.5. Biodegradability

The results obtained after soil burial test are expressed as weight loss vs. time, and illustrated in Fig. 7 A and B. Particularly, in Fig. 7A, the results obtained after each week for composites containing different amounts of laccase-assisted HBA are reported in comparison to the pristine base material *i.e.*, P(3HB)-EC. More specifically, after 4 weeks of burial all of the test composites undergo a faster degradation with respect to the composites containing higher HBA and FA concentration. This behaviour can be well-explained taking into account the results of the swelling ratio from the grafting parameters test that have demonstrated the high swelling linked to the water absorption capacity of the composites. Therefore it seems evident that the swelling capability linked to the water absorption capacity plays a crucial role by causing the hydrolysis of surfaces and interfaces to determine the degradation kinetics of the composites [26, 27]. Whereas, a lower swelling ratio or lower water absorption capacity of the test composites induces a decrease of the soil burial degradation rate [28, 29]. It has already been well-documented in literature that the degradation capability of various cellulolytic organisms, from the soil, to degrade cellulose or cellulose based composite varies greatly with the physicochemical characteristics [15, 30].

4. Conclusions

In conclusion, the newly synthesised laccase-assisted graft composites illustrated a noteworthy biocompatibility characteristics along with their HBA and FA induced antibacterial potential, thus HBA-*g*-P(3HB)-EC and FA-*g*-P(3HB)-EC bio-composites have considerable potential to be used for bio-medical type applications particularly in the area of infection free wound healing, tissue engineering/implants.

Acknowledgements

This work was supported by the Cavendish Research Scholarship program of the University of Westminster, a specialised Doctoral Program for the University of Westminster Scholars. On providing the financial support and laboratory facilities for this study, the University of Westminster is thankfully acknowledged.

References

[1] G. Desmet, E. Taka´cs, L. Wojna´rovits, J. Borsa, Cellulose functionalization via high-energy irradiation-initiated grafting of glycidyl methacrylate and cyclodextrin immobilization, Radiat. Phys. Chem. 80 (2011) 1358-1362.

[2] A. Fillat, O .Gallardo, T .Vidal, F.I.J. Pastor, P. Díaz, M.B. Roncero, Enzymatic grafting of natural phenols to flax fibres: Development of antimicrobial properties, Carbohydr. Polym. 87 (2012) 146-152.

[3] H.M.N. Iqbal, G. Kyazze, T. Tron, T. Keshavarz, A preliminary study on the development and characterisation of enzymatically grafted P (3HB)-ethyl cellulose based novel composites, Cellulose 21 (2014) 3613-3621.

[4] E. Aracri, A. Fillat, J.F. Colom, A. Gutiérrez, J.C. del Río, Á.T. Martínez, Enzymatic grafting of simple phenols on flax and sisal pulp fibres using laccases, Bioresour. Technol. 101 (2010) 8211-8216.

[5] E.M. Cadena, X. Du, G. Gellerstedt, J. Li, A Fillat, J. García-Ubasart, On hexenuronic acid (HexA) removal and mediator coupling to pulp fiber in the laccase/mediator treatment, Bioresour Technol 102 (2011) 3911-3917.

[6] M. Božič, S. Gorgieva, V. Kokol, Homogeneous and heterogeneous methods for laccase-mediated functionalization of chitosan by tannic acid and quercetin, Carbohydr. Polym. 89 (2012) 854-864.

[7] H.M.N. Iqbal, G. Kyazze, T. Tron, T. Keshavarz, Laccase-assisted grafting of poly (3-hydroxybutyrate) onto the bacterial cellulose as backbone polymer: Development and characterisation, Carbohydr. Polym. 113 (2014) 131-137.

[8] H.M.N. Iqbal, G. Kyazze, T. Tron, T. Keshavarz, Laccase-assisted approach to graft multifunctional materials of interest: keratin-EC based novel composites and their characterisation, Macromol. Mater. Eng. 300 (2015) 712-720.

[9] K.K.Y. Wong, J.D. Richardson, S.D. Mansfield, Enzymatic treatment of mechanical pulp for improving papermaking properties, Biotechnol. Prog.16 (2000) 1025-1029.

[10] C. Felby, J. Hassingboe, M. Lund, Pilote-scale production of fibreboard made by laccase oxidized wood fibers: board properties and evidence for crosslinking of lignin, Enzyme Microb. Technol. 31 (2002) 736-741.

[11] G. Elegir, A. Kindl, P. Sadocci, M. Orlandi, Development of antimicrobial cellulose packaging through laccase-mediated grafting of phenolic compounds, Enzyme Microb. Technol. 43 (2008) 84-92.

[12] R.P. Chandra, L.K. Lehtonen, A.J. Ragauskas, Modification of high lignin content kraft pulps with laccase to improve paper strength properties. 1. Laccase treatment in the presence of gallic acid, Biotechnol. Prog. 20 (2004) 255-261.

[13] S. Shahidi, A. Rashidi, M. Ghoranneviss, Investigation of metal absorption and antibacterial activity on cotton fabric modified by low temperature plasma, Cellulose 17 (2010) 627.

[14]S. Shahidi, N. Aslan, M. Ghoranneviss, M. Korachi, Effect of thymol on the antibacterial efficiency of plasma-treated cotton fabric, Cellulose 21 (2014) 1933-1943.

[15]H.M.N. Iqbal, G. Kyazze, I.C. Locke, T. Tron, T. Keshavarz, *In situ* development of self-defensive antibacterial biomaterials: phenol-*g*-keratin-EC based bio-composites with characteristics for biomedical applications, Green Chem. 17 (2015) 3858-3869.

[16]A. Wattanakornsiri, K. Pachana, S. Kaewpirom, M. Traina, C. Migliaresi, Preparation and properties of green composites based on tapioca starch and differently recycled paper cellulose fibers, J. Polym. Environ. 20 (2012) 801-809.

[17]E. Smith, G. Dent, in: Modern Raman Spectroscopy. A Practical Approach, (2005) J. Wiley & Sons, Ltd., Chinchester.

[18]K. Yamada, T. Abe, Y. Tanizawa, Black tea stain formed on the surface of teacups and pots. Part 2—Study of the structure change caused by aging and calcium addition, Food Chem. 103 (2007) 8-14.

[19]T. Sun, P. Xu, Q. Liu, J. Xue, W. Xie, Graft copolymerization of methacrylic acid onto carboxymethyl chitosan, Eur. Polym. J. 39 (2003) 189-192.

[20]G. Kumar, P.J. Smith, G.F. Payne, Enzymatic grafting of a natural product onto chitosan to confer water solubility under basic conditions, Biotechnol. Bioeng. 63 (1999) 154-165.

[21]T. Chen, G. Kumar, M.T. Harris, P.J. Smith, G.F. Payne, Enzymatic grafting of hexyloxyphenol onto chitosan to alter surface and rheological properties, Biotechnol. Bioeng. 70 (2000) 564-573.

[22]Y.A. Aggour, Reaction kinetics of graft copolymerization and thermochemical studies of the degradation of poly(vinyl alcohol) graft copolymer, Polym. Int. 50 (2001) 347-353.

[23]S. Li, N. Jia, M. Ma, Z. Zhang, Q. Liu, R. Sun, Cellulose-silver nanocomposites: microwave-assisted synthesis, characterization, their thermal stability, and antimicrobial property, Carbohydr. Polym. 86 (2011) 441-447.

[24]C. Dong, Y. Ye, L. Qian, G. Zhao, B. He, H. Xiao, Antibacterial modification of cellulose fibers by grafting β-cyclodextrin and inclusion with ciprofloxacin, Cellulose 21 (2014) 1921-1932.

[25]A. Ultee, M.H.J. Bennik, R. Moezelaar, The phenolic hydroxyl group of carvacol is essential for action against the food-borne pathogen *Bacillis cereus*, Appl. Environ. Microbiol. 68 (2002) 1561-1568.

[26]A.C. Vieira, J.C. Vieira, J.M. Ferra, Mechanical study of PLA–PCL fibers during in vitro degradation, J. Mech. Behav. Biomed. Mater. 4 (2011) 451-460.

[27]W.L. Tham, Z.A. Mohd Ishak, W.S. Chow, Water absorption and hygrothermal aging behaviors of SEBSg-MAH toughened poly(lactic acid)/halloysite nanocomposites, Polym. Plast. Technol. Eng. 53 (2014) 472-480.

[28]V.A. Alvarez, R.A. Ruseckaite, A. Vazquez, Degradation of sisal fibre/Mater Bi-Y biocomposites buried in soil, Polym. Degrad. Stab. 91 (2006) 3156-3162.

[29]M. Cocca, R. Avolio, G. Gentile, E. Di Pace, M.E. Errico, M. Avella, Amorphized cellulose as filler in biocomposites based on poly (ε-caprolactone), Carbohydr. Polym. 118 (2015) 170-182.

[30]Y. Amano, K. Nozaki, T. Araki, H. Shibasaki, S. Kuga, T. Kanda, Reactivities of cellulases from fungi towards ribbon-type bacterial cellulose and band-shaped bacterial cellulose, Cellulose 8 (2001) 267-274.

Figure captions

Figure 1 FT-IR spectra: **(A)** HBA and HBA-*g*-P(3HB)-EC bio-composites *i.e.,* 0HBA-*g*-P(3HB)-EC, 5HBA-*g*-P(3HB)-EC, 10HBA-*g*-P(3HB)-EC, 15HBA-*g*-P(3HB)-EC and 20HBA-*g*-P(3HB)-EC and **(B)** FA and FA-*g*-P(3HB)-EC bio-composites *i.e.,* 0FA-*g*-P(3HB)-EC, 5FA-*g*-P(3HB)-EC, 10FA-*g*-P(3HB)-EC, 15FA-*g*-P(3HB)-EC and 20FA-*g*-P(3HB)-EC.

Figure 2 Graft yield (%GY), grafting efficiency (%GE) and swelling ratio (%SR) behaviours of HBA-*g*-P(3HB)-EC bio-composites (**A**) and FA-*g*-P(3HB)-EC bio-composites (**B**).

Figure 3 Antibacterial activities of HBA-*g*-P(3HB)-EC bio-composites (**A**) and FA-*g*-P(3HB)-EC bio-composites (**B**) against *B. subtilis* NCTC 3610 and *E. coli* NTCT 10418.

Figure 4 Neutral red dye concentration dependent percentage cell viability of human keratinocytes-like HaCaT cells after 1, 3 and 5 days of incubation on the HBA-*g*-P(3HB)-*g*-EC bio-composites (**A**) and FA-*g*-P(3HB)-*g*-EC bio-composites (**B**), (mean ± SD, n = 3).

Figure 5 Adherent morphology of stained images of HaCaT cells seeded on the HBA-*g*-P(3HB)-EC bio-composites. Images A, B and C represent the HaCaT cells on native P(3HB)-EC (*i.e.,* 0HBA-*g*-P(3HB)-EC) after 1, 3 and 5 days of incubation, respectively; images D, E and F represent the adhered HaCaT cells on 5HBA-*g*-P(3HB)-EC after 1, 3 and 5 days of incubation, respectively; images G, H and I represent the adhered HaCaT cells on 10HBA-*g*-P(3HB)-EC after 1, 3 and 5 days of incubation, respectively; images J, K and L represent the adhered HaCaT cells on 15HBA-*g*-P(3HB)-EC after 1, 3 and 5 days of incubation, respectively and images M, N and O represent the adhered HaCaT cells on 20HBA-*g*-P(3HB)-EC after 1, 3 and 5 days of incubation, respectively. All images from A-O were taken at 100× magnification whereas, A*-O* are magnified images of A-O.

Figure 6 Adherent morphology of stained images of HaCaT cells seeded on the FA-*g*-P(3HB)-EC bio-composites. Images A, B and C represent the HaCaT cells on native P(3HB)-EC (*i.e.,* 0FA-*g*-P(3HB)-EC) after 1, 3 and 5 days of incubation, respectively; images D, E and F represent the adhered HaCaT cells on 5FA-*g*-P(3HB)-EC after 1, 3 and 5 days of incubation, respectively; images G, H and I represent the adhered HaCaT cells on 10FA-*g*-P(3HB)-EC after 1, 3 and 5 days of incubation, respectively; images J, K and L represent the adhered HaCaT cells on 15FA-*g*-P(3HB)-EC after 1, 3 and 5 days of incubation, respectively and images M, N and O represent the adhered HaCaT cells on 20FA-*g*-P(3HB)-EC after 1, 3 and 5 days of incubation, respectively. All images from A-O were taken at 100× magnification whereas, A*-O* are magnified images of A-O.

Figure 7 Biodegradability of HBA-*g*-P(3HB)-EC bio-composites (**A**) and FA-*g*-P(3HB)-*g*-EC bio-composites (**B**) buried in soil for prescribed time periods, (mean ± SD, n = 3).

List of Figures

Fig. 1

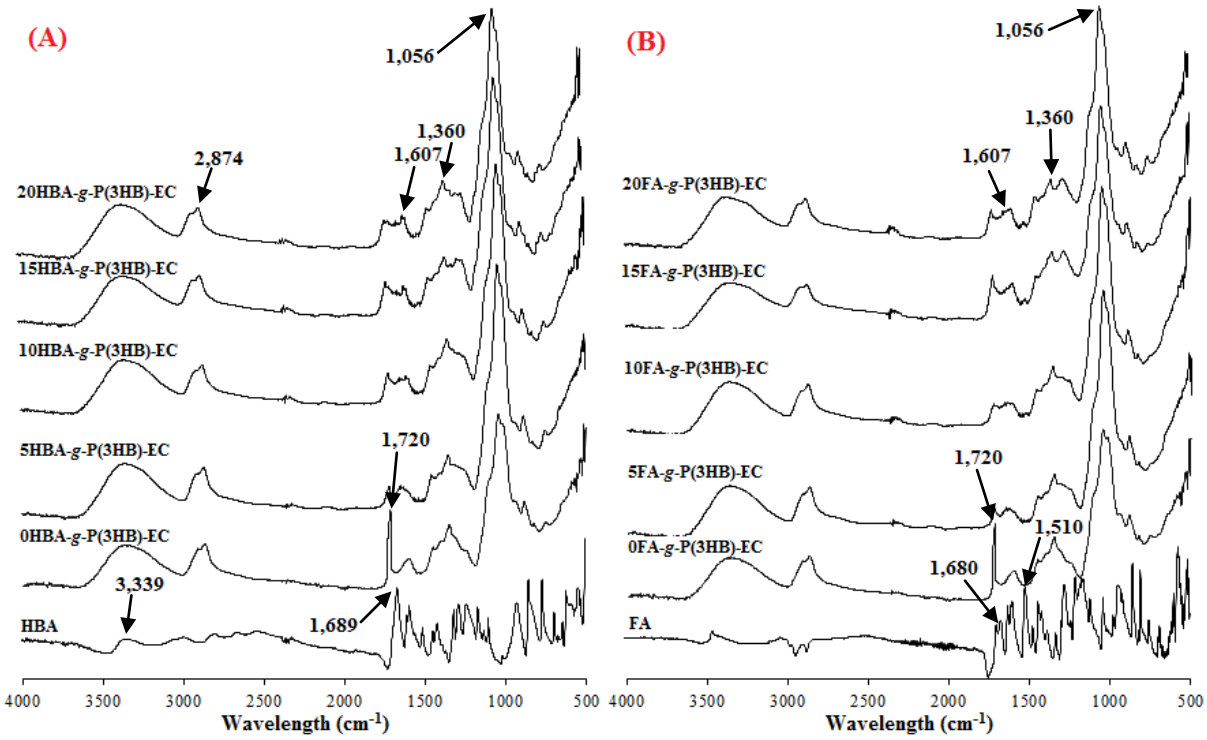

Fig. 2

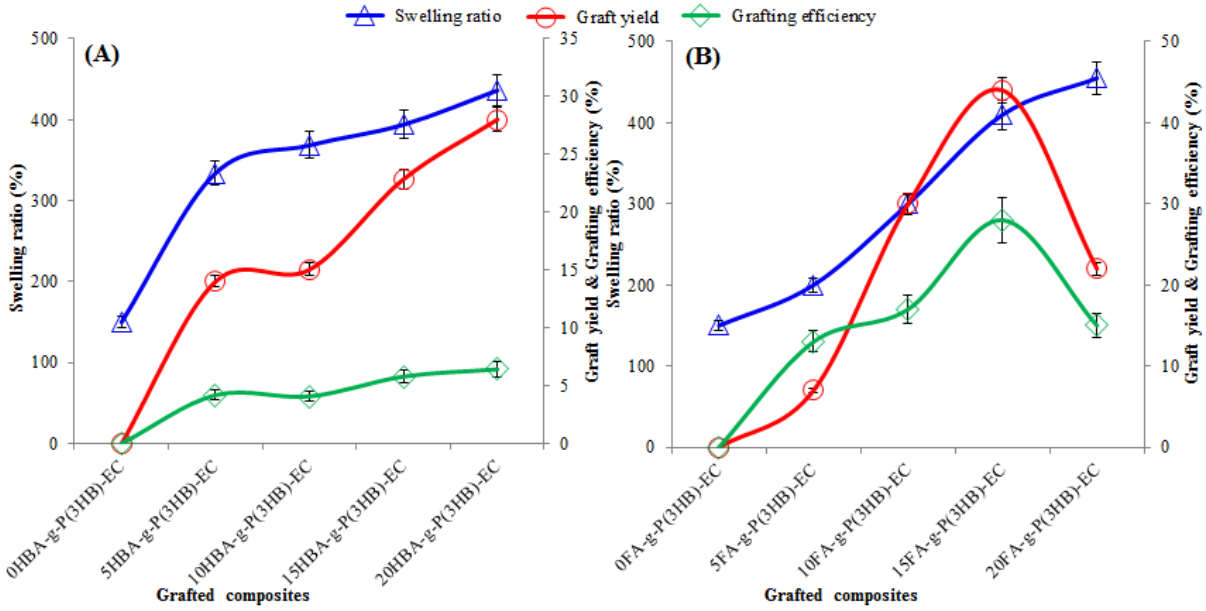
Swelling ratio
Graft yield
Grafting efficiency
(A)
(B)
Swelling ratio (%)
Graft yield & Grafting efficiency (%)
0HBA-g-P(3HB)-EC
5HBA-g-P(3HB)-EC
10HBA-g-P(3HB)-EC
15HBA-g-P(3HB)-EC
20HBA-g-P(3HB)-EC
0FA-g-P(3HB)-EC
5FA-g-P(3HB)-EC
10FA-g-P(3HB)-EC
15FA-g-P(3HB)-EC
20FA-g-P(3HB)-EC
Grafted composites

Fig. 3

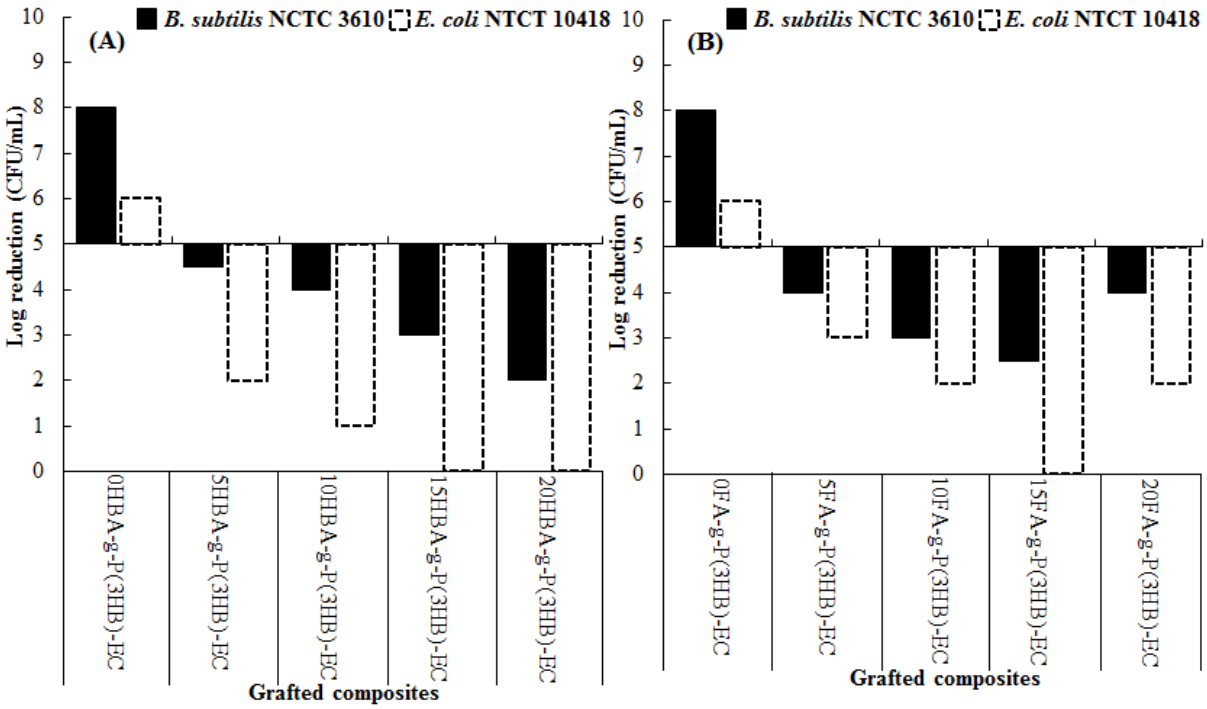
(A)
B. subtilis NCTC 3610
E. coli NTCT 10418
Log reduction (CFU/mL)
0
1
2
3
4
5
6
7
8
9
10
0HBA-g-P(3HB)-EC
5HBA-g-P(3HB)-EC
10HBA-g-P(3HB)-EC
15HBA-g-P(3HB)-EC
20HBA-g-P(3HB)-EC
Grafted composites
(B)
B. subtilis NCTC 3610
E. coli NTCT 10418
Log reduction (CFU/mL)
0FA-g-P(3HB)-EC
5FA-g-P(3HB)-EC
10FA-g-P(3HB)-EC
15FA-g-P(3HB)-EC
20FA-g-P(3HB)-EC
Grafted composites

Fig. 4

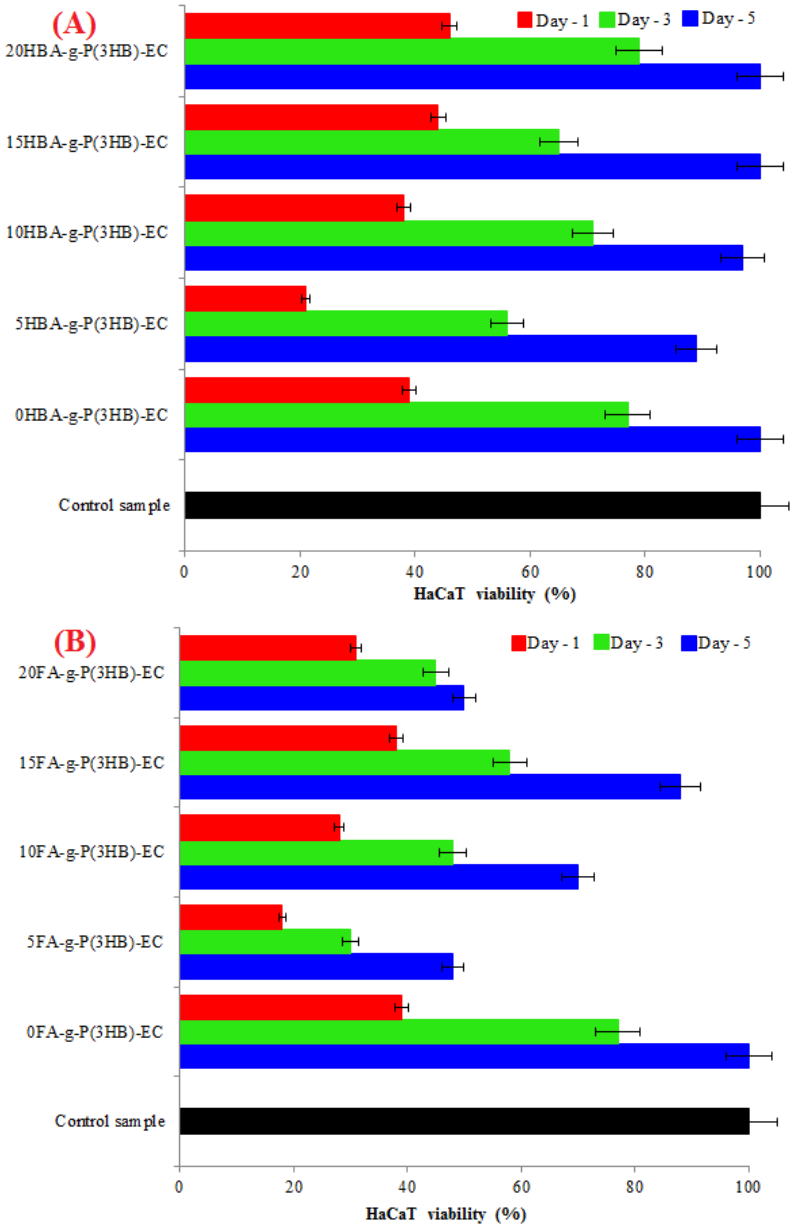
(A)
Day - 1
Day - 3
Day - 5
20HBA-g-P(3HB)-EC
15HBA-g-P(3HB)-EC
10HBA-g-P(3HB)-EC
5HBA-g-P(3HB)-EC
0HBA-g-P(3HB)-EC
Control sample
0
20
40
60
80
100
HaCaT viability (%)
(B)
Day - 1
Day - 3
Day - 5
20FA-g-P(3HB)-EC
15FA-g-P(3HB)-EC
10FA-g-P(3HB)-EC
5FA-g-P(3HB)-EC
0FA-g-P(3HB)-EC
Control sample
0
20
40
60
80
100
HaCaT viability (%)

Fig. 5

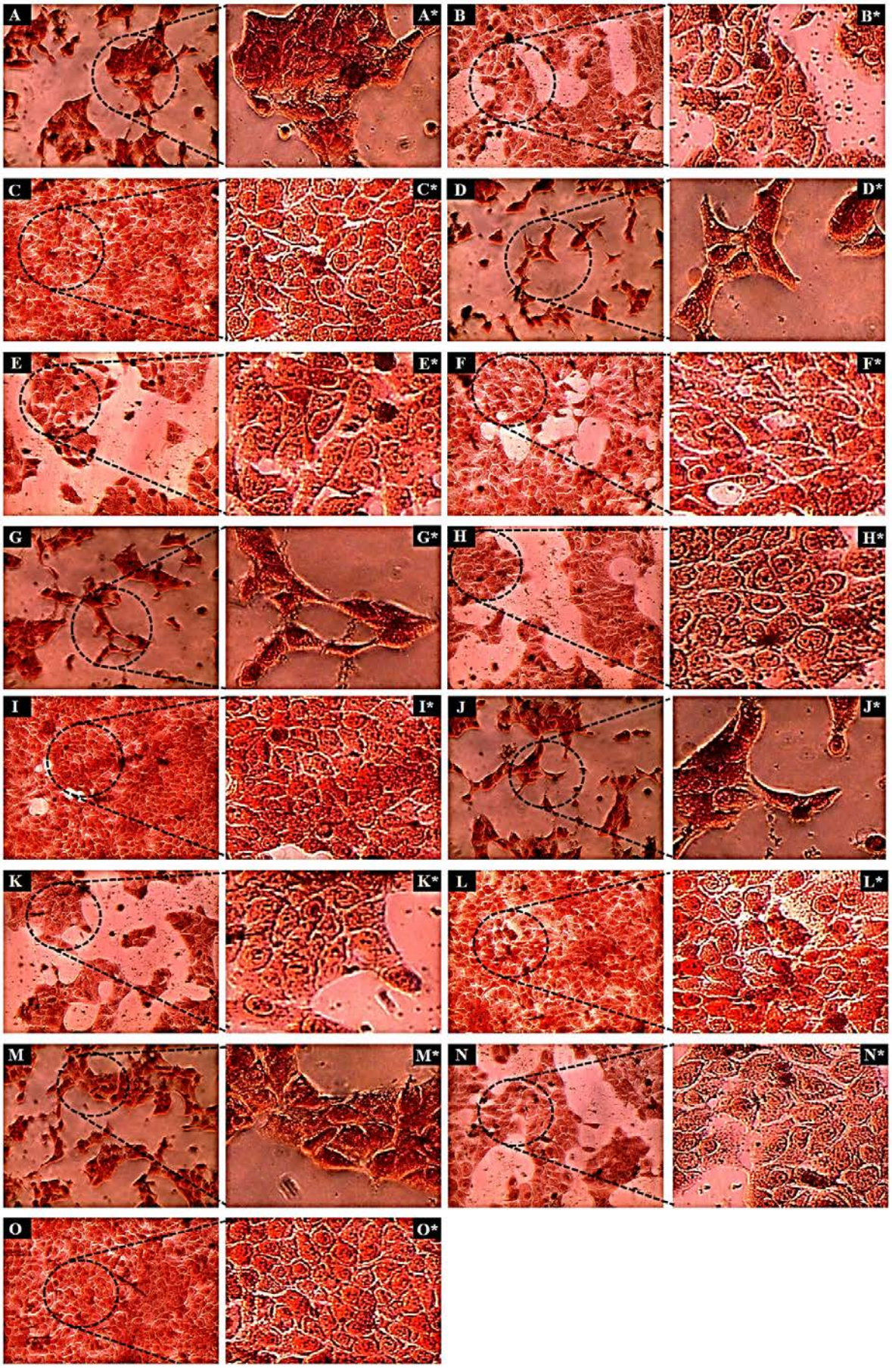

Fig. 6

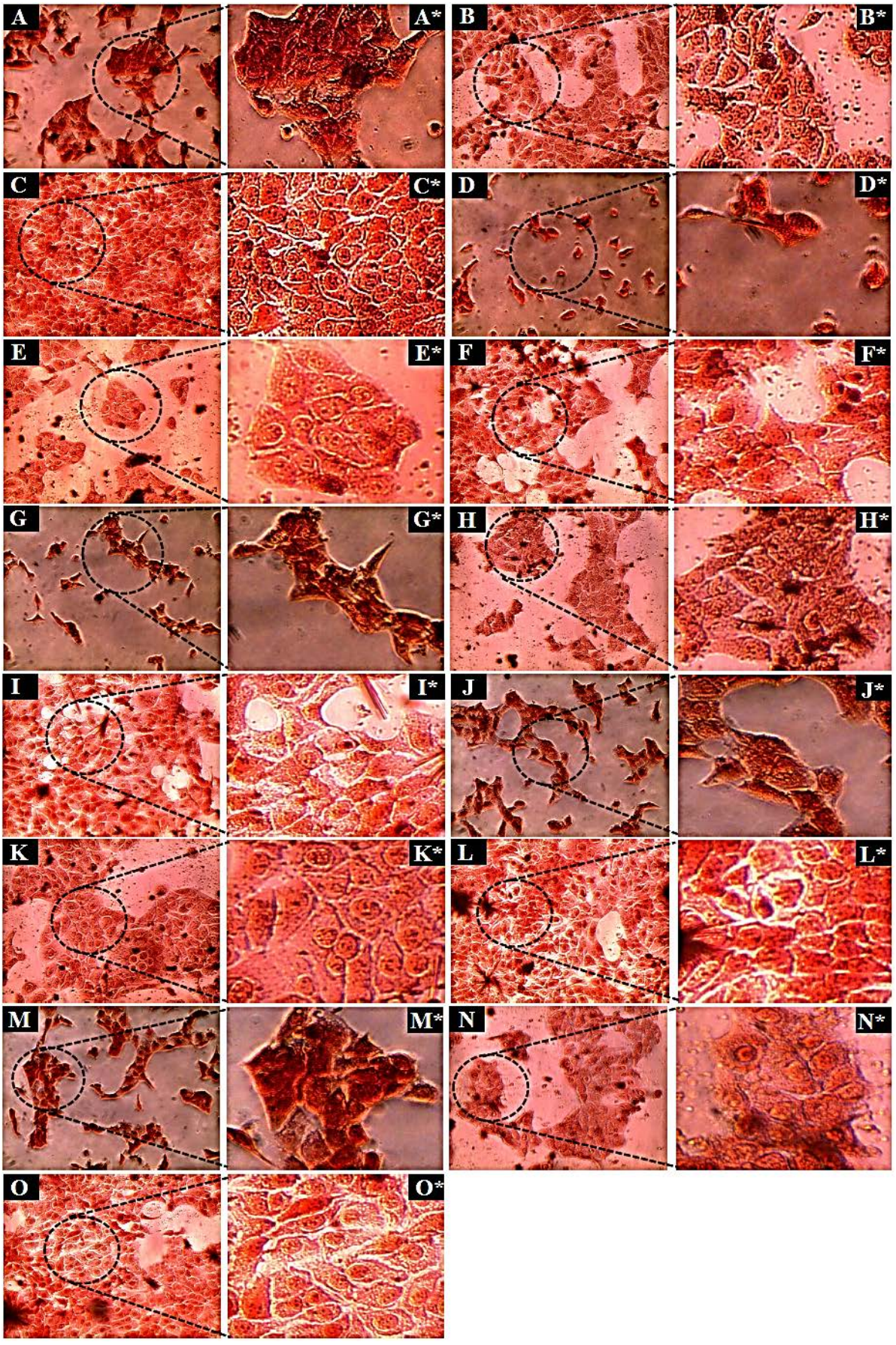

Fig. 7

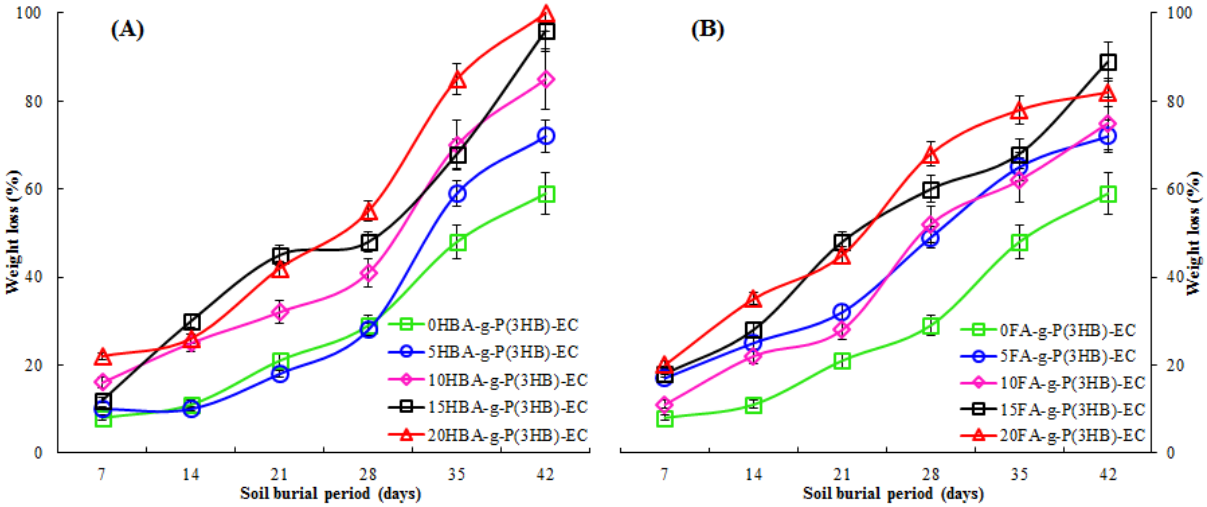
(A)
(B)
Weight loss (%)
Soil burial period (days)
0HBA-g-P(3HB)-EC
5HBA-g-P(3HB)-EC
10HBA-g-P(3HB)-EC
15HBA-g-P(3HB)-EC
20HBA-g-P(3HB)-EC
0FA-g-P(3HB)-EC
5FA-g-P(3HB)-EC
10FA-g-P(3HB)-EC
15FA-g-P(3HB)-EC
20FA-g-P(3HB)-EC